



[View PDF Version](#)[Previous Article](#)[Next Article](#)

DOI: [10.1039/D1OB01791H](https://doi.org/10.1039/D1OB01791H) (Communication) *Org. Biomol. Chem.*, 2022, **20**, 98-105

Pyrrovobasine, hybrid alkylated pyrrolidine monoterpene indole alkaloid pseudodimer discovered using a combination of mass spectral and NMR-based machine learning annotations[†]

Hugues Fouotsa ^{abc}, Pierre Mkounga ^c, Alain Meli Lannang ^d, Jérôme Vanheuverzwijn ^b, Zhiyu Zhou ^b, Karine Leblanc ^a, Somia Rharrabti ^a, Augustin Ephrem Nkengfack ^c, Jean-François Gallard ^e, Véronique Fontaine ^b, Franck Meyer ^b, Erwan Poupon ^a, Pierre Le Pogam ^{*a} and Mehdi A. Beniddir ^{*a}

^aÉquipe “Chimie des Substances Naturelles” Université Paris-Saclay, CNRS, BioCIS, 5 rue J.-B. Clément, 92290 Châtenay-Malabry, France.

E-mail: pierre.le-pogam-alluard@universite-paris-saclay.fr; mehdi.beniddir@universite-paris-saclay.fr

^bFaculty of Pharmacy, Microbiology, Bioorganic and Macromolecular Chemistry Unit, Université Libre de Bruxelles, Campus de la Plaine-CP 206/04, Boulevard du Triomphe, ACC.2, Po Box 1050, Belgium

^cDepartment of Organic Chemistry, Faculty of Science, University of Yaoundé I, P.O. Box 812, Yaoundé, Cameroon

^dDepartment of Chemistry, Higher Teachers Training College, University of Maroua, P.O. Box 55, Maroua, Cameroon

^eInstitut de Chimie des Substances Naturelles, CNRS, ICSN UPR 2301, Université Paris-Saclay, 91198 Gif-sur-Yvette, France

Received 12th September 2021 , Accepted 27th September 2021

First published on 27th September 2021

Abstract

A new vobasine–tryptamine-based monoterpene indole alkaloid pseudodimer was isolated from the stem bark of *Voacanga africana*. As a minor constituent occurring in a thoroughly investigated plant, this molecule was targeted based on a molecular networking strategy and a rational MS²-guided phytochemical investigation led to its isolation. Its structure was formally established based on HRMS, 1D/2D NMR data, and the application of the tool Small Molecule Accurate Recognition Technology (SMART 2.0). Its absolute configuration was assigned by the exciton chirality method and TD-DFT ECD calculations. Besides featuring an unprecedented intermonomeric linkage in the small group of vobasine/tryptamine hybrids, pyrrovobasine also represents the first pyrrolidine-containing representative in the whole monoterpene indole alkaloids group. Biosynthetic hypotheses possibly underpinning these structural oddities are proposed here.

Introduction

Fueled by the diverse ethnopharmacological claims related to *Voacanga africana* Stapf ex Scott-Elliott, decades of intensive phytochemical campaigns unveiled the array of specialized products it shelters with a salient emphasis on its monoterpene indole

alkaloid (MIA) content. Notwithstanding the long-held interest in *V. africana* chemistry, new appendages of MIAs are continuously being reported from this plant source.¹⁻³ The tremendous advances in MS²-based data processing strategies and in sensitivity of NMR techniques provide natural product chemists with ever-expanding capabilities for exploration of compounds occurring in minute amounts.^{4,5} These refined analytical workflows pave the way for the re-investigation of deeply dug models using a state-of-the-art pipeline to gear the isolation efforts towards so-far overlooked chemical entities.⁶⁻¹² In the frame of our quest for new MIA-type specialized metabolites, and benefitting from our recent upload to the GNPS spectral libraries of the MIADB,¹³ we embarked on a molecular-networking-based phytochemical investigation of *V. africana* stem bark. The observation of a molecular family clustered around a node tentatively tagged as ceridimine, a rare vobasine/tryptamine-type pseudodimer so far only known from *Pagiantha cerifera* (Pancher & Sebert) Markgr.,¹⁴ sparked our interest and guided us to isolate the newly-reported pyrrovobasine (**1**) following a MS²-streamlined isolation workflow. Besides representing the first instance of vobasine–tryptamine dimer featuring a C-3–C-2' interunit bonding,^{15,16} pyrrovobasine is also the first pyrrolidine-containing member in the huge phytochemical class of MIAs.

Results and discussion

To reach a wide and untargeted insight into the indolomonoterpenic alkaloid content of *V. africana*, both the alkaloid and crude ethanolic extracts of its stem bark were profiled by HPLC-HRMS² (positive polarity). These data were subsequently processed using the classical molecular-networking workflow¹⁷ and dereplicated against the MIADB-implemented GNPS spectral libraries. A cautious examination of the obtained molecular network (Fig. S1†) highlighted a molecular family consisting of four nodes (Fig. S2†) instigating a connection with a central node tentatively tagged as ceridimine. This constellation held a peculiar significance as only very few derivatives of ceridimine,¹⁴ pertaining to the rare phytochemical class of vobasine–tryptamine pseudodimers, have been reported so far with none being consistent with the currently disclosed nominal masses. With this in mind, the LC-DAD-MS profile related to the alkaloidal extract of *V. africana* was monitored to check which of these compounds could be isolated in sufficient yield for full structure elucidation, leading us to guide our

isolation efforts towards the ion detected at m/z 605.303. Notwithstanding its relatively elevated molecular mass, the mass spectrum of this compound lacked the diagnostic isotopic pattern for doubly charged ion species encountered in most dimeric monoterpene indole alkaloids. This observation hinted that this molecule comprises a unique basic site, which strengthened our interest in isolating it. The molecular formula retrieved from this mass spectrometric signal, $C_{37}H_{40}N_4O_4$, returned no hit in the *Dictionary of Natural Products*,¹⁸ deftly convincing us to undertake its MS²-streamlined isolation.

Compound **1** ([Fig. 1](#)) was isolated from the alkaloidic extract of *V. africana* stem bark by repetitive chromatographic separations following a MS²-guided phytochemical pipeline. Obtained as a brown amorphous solid, its molecular formula was confirmed to be $C_{37}H_{40}N_4O_4$ based on the protonated molecular ion at m/z 605.3122 (calcd for $C_{37}H_{41}N_4O_4$, 605.3122), indicating 20 degrees of hydrogen deficiency. The cursory examination of the NMR data of **1** revealed NMR landmarks evocative of a 3-vobasiny unit.¹⁹ Accordingly, the ¹H and ¹³C NMR data of **1** showcased the presence of four aromatic resonances, an upfield-shifted methyl ester group (δ_H 2.49/ δ_C 169.2; 51.0), an *N*₄-Me group (δ_H 2.89/ δ_C 40.5) and an ethylidene side chain (δ_H 5.60/ δ_C 126.6; δ_H 1.73/ δ_C 13.0). Alongside the crosspeaks related to the contiguous aromatic hydrogens of the indole core, the COSY spectrum confirmed the occurrence of an isolated aminomethylene (C-21), of an ethylidene fragment, and of an extended CH₂CHCHCH₂CH spin system, displaying chemical shifts diagnostic of the C₆-C₅-C₁₆-C₁₅-C₁₄-C₃ appendage of a vobasine-type MIA, further validated by the key HMBC crosspeaks outlined in [Fig. 2B](#). The shielded chemical shift of the ester methyl linked to C-16 placed it within the shielding zone of the indole nucleus.⁶

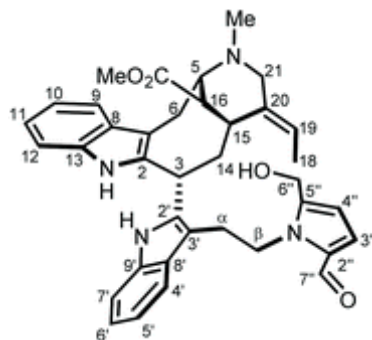


Fig. 1 Chemical structure of pyrrovobasine (**1**).

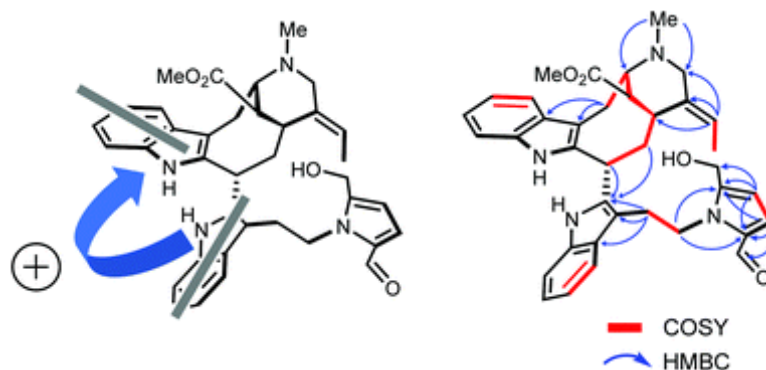


Fig. 2 (A) Two electronic dipoles denoting a positive chirality. (B) Selected 2D NMR correlations for **1**.

Consistent with the molecular network which determined **1** as a close derivative of ceridimine, the remaining signals hinted the occurrence of an additional free side chain-bearing tryptamine unit. Four additional resonances related to aromatic/olefinic protons substantiated this assumption, as well as the two vicinal methylenic protons that determined a $\text{CH}_2\text{CH}_2\text{N}$ fragment. The structural

elements elucidated so far determined **1** as a vobasine–tryptamine pseudodimer. This small phytochemical class is so far represented by three molecules, all obtained from an apocynaceous source: ceridimine (from *P. cerifera*),¹⁴ demethylceridimine (from the by-then *Peschiera buchtienii* (H.J.P.Winkl.) Markgr.,²⁰ now known as *Tabernaemontana cymosa* Jacq.), and hunteriatryptamine (from *Hunteria zeylanica* (Retz.) Gardner ex Thwaites).²¹ All these closely related molecules featured a linkage between the C-3 position of the vobasinyl residue to the C-6' site of the tryptamine component. Regarding **1**, the HMBC correlations from the protons resonating at δ_{H} 2.02 (H-14), at δ_{H} 4.87 (H-3), and at δ_{H} 3.42 (H₂- α) to C-2' (δ_{C} 137.9) were diagnostic of a so-far unprecedented C-3–C-2' connection between the vobasine and tryptamine units. The β -orientation of H-3 was established based on the magnitude of the coupling constant values (dd, J = 13.4, 2.7 Hz), in excellent agreement with former literature reports.²²

At this stage of the structure elucidation process, a few signal patterns were still pending assignment: two contiguous aromatic/olefinic protons disclosing an unusual coupling constant value of 3.9 Hz [δ_{H} 6.97 (1H, d, J = 3.9 Hz)/ δ_{C} 124.3; δ_{H} 6.30 (1H, d, J = 3.9 Hz)/ δ_{C} 110.7], a shielded aldehydic proton [δ_{H} 9.56 (1H, s)/ δ_{C} 179.9], a set of oxygenated methylenic protons [δ_{H} 4.63 (1H, d, J = 13.5 Hz) and 4.77 (1H, d, J = 13.5 Hz)/ δ_{C} 56.7], and finally two low-field shifted quaternary carbons (δ_{C} 141.9 and 132.9). To expedite the elucidation of this specific fragment, the HSQC data retrieved from it were collated in a .csv file prior to being uploaded into the SMART 2.0 (Small Molecule Accurate Recognition Technology) platform. This artificial intelligence-based tool is used to generate structure hypotheses from HSQC data through a deep convolutional neural network architecture that includes the ¹H–¹³C HSQC spectra related to more than 53 000 natural products (encompassing approximately 15% of the known natural products as of 2020).^{23,24} SMART analysis revealed 5-(hydroxymethyl)pyrrole-2-carbaldehyde, or pyrraline, to be the preferred hit (cosine value \approx 0.97), guiding us to consider it to account for the so far unassigned structural elements. Accordingly, SMART assistance tended to elucidate the structure of **1** as indicated in [Fig. 1](#), in good agreement with molecular formula requirements. The key HMBC correlations outlined in [Fig. 2B](#) confirmed this tentative structure as the nitrogen atom of the pyrrole nucleus was shown to correspond to that of the side chain of the tryptamine unit, as evidenced based on the HMBC correlations from the protons resonating at δ_{H} 4.84 (H₂- β) to both C-2'' (δ_{C} 132.9) and C-5'' (δ_{C} 141.9). A

rapid literature survey indicated that pyrroline-containing natural products display highly similar chemical shifts values, also for aromatic quaternaries left unconsidered throughout SMART analyses.²⁵ The absolute configuration of **1** was determined using the exciton chirality CD method.²⁶ The positive sign of the first Cotton effect [λ_{max} 237 nm ($\Delta\epsilon + 31$)] and the negative sign of the second one [λ_{max} 222 nm ($\Delta\epsilon - 21$)] (Fig. 3) indicated a right-handed screw between the two indole chromophores (Fig. 2A).²⁷ The good fit between the calculated ECD spectrum of the lowest-energy conformer of **1** and the experimental ECD spectrum confirmed the proposed absolute configuration (Fig. 3). These structural features allowed to elucidate the structure of **1**, namely pyrovobasine, as shown in Fig. 1.

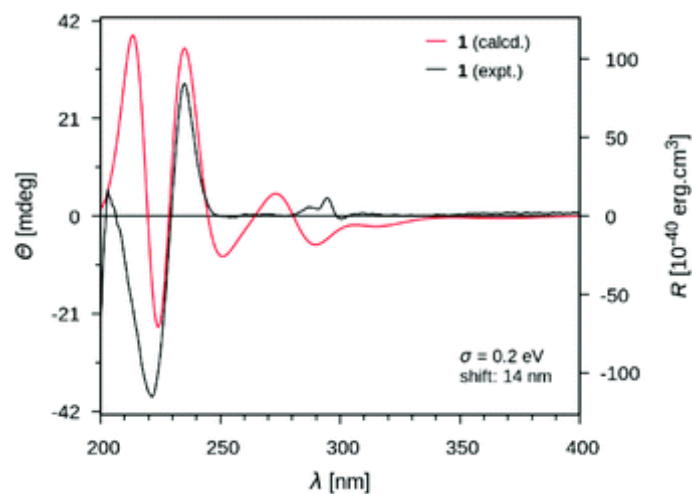


Fig. 3 ECD spectra of **1** (experimental and calculated at the B3LYP/6-31G* level).

Pyrovobasine features several structural oddities which are worth being stressed out. As already pinpointed, the nature of the connection between the tryptamine and the vobasine subunits meets no precedents in this small group of pseudodimers. The electrophilic nature of vobasinol C-3 (Fig. 4) is illustrious and, as such, dimeric MIA structures disclosing a 3-vobasiny residue following its

attack by an electron-rich center are of considerable generality.¹⁵ As per the tryptamine component, a literature survey indicates that an array of different substituents can be encountered at a tryptaminic C-2 position such as prenyl groups,²⁸ bromine atoms,²⁹ methyl groups,³⁰ a beta-carboline,³¹ or may even lead to disulfide-bonded dimeric structures.³² The depiction of the resonance contributors related to the indolic system reveals that all non-bridgehead carbons can serve as functional carbanion equivalents.^{33,34}

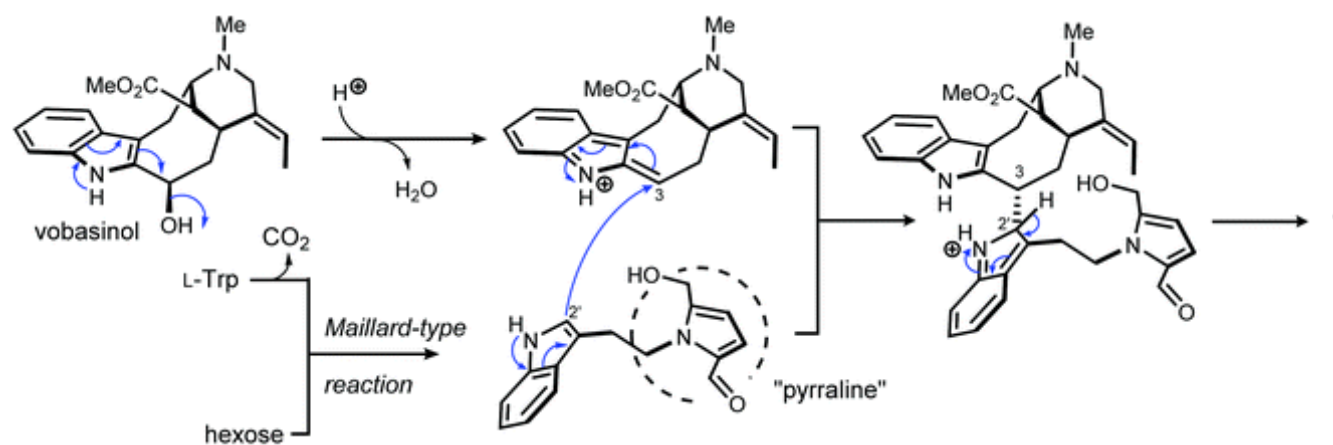


Fig. 4 Possible biosynthetic logic of pyrrovobasine (1).

At last, 5-hydroxymethylpyrrole-2-carbaldehyde, sometimes referred to as pyrraline, is known from a wealth of natural sources, but also from cooked foods.³⁵ No enzymatic biosynthetic pathway to this nucleus has been proposed so far and it is rather believed that this ring system arises by condensation of amines and sugars, following the so-called Maillard reaction (Fig. 4).³⁶ Consistent with this viewpoint, 2-formylpyrrole-containing natural substances are ubiquitous in nature and these molecules – recently reviewed by Brimble *et al.* are classified based on the nature of their amine component, falling into three major types: amino acids, biogenic amines or amino

sugars.³⁵ Tryptamine-based pyrrole alkaloids have already been reported from macromycetes in particular.^{37,38} Yet, to the best of our knowledge, pyrrovobasine represents the first example of pyrraline-containing monoterpene indole alkaloid.

The *in vitro* antibacterial activities of compound **1** were evaluated against *Mycobacterium smegmatis*, *M. abscessus*, *M. bovis* BCG, *Staphylococcus aureus* and *Pseudomonas aeruginosa*. The results showed that pyrrovobasine (**1**) exerts no antibacterial activity (MIC > 50 µg mL⁻¹).

Conclusions

In summary, we have described the first member of the pyrrovobasine family of natural products from the stem bark of *V. africana*, representing the first example of a pyrraline-containing monoterpene indole alkaloid. The isolation process was enabled by exploiting a molecular networking approach and the structure elucidation was assisted by an NMR-based machine learning tool.

Experimental section

General experimental procedures

Optical rotations were measured at 25 °C on a Polaar 32 polarimeter. UV spectra were recorded on a Lightwave II + WPA 7126 V. 1.6.1 spectrophotometer. ECD spectra were measured at 25 °C on a JASCO J-810 spectropolarimeter. IR spectra were recorded with a PerkinElmer type 257 spectrometer. The NMR spectra were recorded on a Bruker AM-600 (600 MHz) NMR spectrometer equipped with a TCI 5 mm cryoprobe using CDCl₃ as a solvent. The solvent signal was used as a reference. Sunfire preparative C₁₈ columns (150 × 19 mm, i.d. 5 µm and 150 × 30 mm, i.d. 5 µm; Waters) were used for preparative HPLC separations using a Waters Delta Prep equipped with a binary pump (Waters 2525) and a UV-visible diode array detector (190–600 nm, Waters 2996). Silica 330 g, 120 g, and 24 g Grace cartridges were used for flash chromatography using an Armen Instrument spot liquid chromatography flash apparatus. Chemicals and solvents were purchased from Sigma-Aldrich.

Plant material

The fresh bark of *V. africana* (Yaounde National Herbarium voucher specimen No. HNY/1949; Victor Nana (collector)) was collected from the campus of the University of Yaounde I, Cameroon in December 2019.

Extraction and isolation

The air-dried and powdered bark of *V. africana* (2.3 kg) was extracted three times with MeOH at room temperature. The resulting extract was concentrated under reduced pressure to obtain a crude extract (231 g). The obtain extract was dissolved in the mixture MeOH–H₂O 10% and alkalinized with NH₃ (pH = 12) and extracted with CH₂Cl₂ (3 × 1.5 L, 1 h each, 20 °C, atmospheric pressure). The mixture was concentrated under vacuum at 38 °C to yield 50.5 g of an alkaloid extract. A part of this residue (VADCM, 25 g) was subjected to flash chromatography using a silica 330 g Grace cartridge with a gradient of CH₂Cl₂–MeOH (100 : 0 to 0 : 100) at 80 mL min⁻¹ to afford fifteen fractions, VA1–VA15, according to their TLC profiles. Fractions VA4–VA6 were gathered (14.7 g) and were subjected to a second flash chromatography using a silica 120 g Grace cartridge with a gradient of CH₂Cl₂–MeOH (100 : 0 to 0 : 100) at 80 mL min⁻¹ to afford thirteen fractions VAB1–VAB13. Among them, VAB6 (1.7 g) was selected for further fractionation and submitted to Sephadex LH20 and eluted with a mixture of MeOH : CH₂Cl₂ (8 : 2) to afford fifteen fractions VAB61–VAB615. VAB67 (761 mg) was submitted again to Sephadex LH-20 (4 cm × 90 cm) and eluted with a mixture of MeOH : CH₂Cl₂ (8 : 2) to afford thirteen fractions VAB671–VAB6713. VAB6713 underwent a preparative HPLC separation using a gradient of MeOH–H₂O with 0.1% formic acid (grad 10–80% in 25 min) to give compound **1** (3.2 mg, yield 0.0005%).

Physical and spectroscopic data of 1

Pyrrrovobasine (1). Brown amorphous solid; $[\alpha]^{25.0}_D + 160$ (*c* 0.05, MeOH); IR ν_{\max} 3400, 1720 cm⁻¹; UV (MeOH) λ_{\max} (log ϵ) 232 (2.42), 296.1 (3.3) nm; ¹H and ¹³C NMR data, see [Table 1](#); HR-ESI-MS *m/z* 605.3122 [M + H]⁺ (calcd for C₃₇H₄₁N₄O₄, 605.3122); MS/MS spectrum was

deposited in the GNPS spectral library under the identifier: CCMSLIB00006710432.

Table 1 ^1H and ^{13}C NMR Data for **1** (CDCl_3 , 600/150 MHz)

No.	δ_{H} , mult		δ_{H} , mult		
	(J, Hz)	δ_{C}	No.	(J, Hz)	δ_{C}
1	8.24, br s		1'	8.30, br	
	(NH)			(NH) s	
2		135.8			
3	4.87, dd	35.8	2'		137.9
	(13.4, 2.7)				
5	4.42, t	60.7	3'		107.6
	(8.5)				
6	3.63, m	21.5	4'	7.72, m	118.9
	3.74, m				
			5'	7.08,	120.0
				ov.	
7		106.8			
8		129.1	6'	7.08,	122.9
				ov.	

No.	δ_H , mult		δ_H , mult		
	(J, Hz)	δ_C	No.	(J, Hz)	δ_C
9	7.55, d (7.7)	117.7			
10	7.11, ov.	120.0	7'	7.16, ov.	110.8
11	7.15, ov.	122.9	8'		128.4
12	7.16, ov.	110.8	9'		135.8
13		136.4	α	3.42, m	26.7
14	2.02, ddd (15.0, 6.7, 3.1) 2.75, q (13.4)	35.2	β	4.67, ov. 4.84, dd (13.7, 6.7)	46.9
15	3.89, m	32.5	2''		132.9
16	2.99, br s	43.8	3''	6.97, d (3.9)	124.3
			4''	6.30, d (3.9)	110.7

$\delta_{\text{H}}, \text{mult}$			$\delta_{\text{H}}, \text{mult}$		
No.	(J, Hz)	δ_{C}	No.	(J, Hz)	δ_{C}
18	1.73, d (6.9)	13.0	5''		141.9
			6''	4.63, d (13.5)	56.7
19	5.60, q (6.9)	126.6		4.67, d (13.5)	
			7''	9.56, s	179.9
20		132.9			
21	4.23, d (13.7)	51.4			
	3.45, ov.				
<u>C</u>		169.2			
OOMe					
COO	2.49, s	51.0			
<u>Me</u>					
N-Me	2.89, s	40.5			

Data dependent LC-HRMS² analyses

LC-ESI-HRMS² analyses were achieved by coupling the LC system to a hybrid quadrupole time of-flight mass spectrometer Agilent 6530 (Agilent Technologies, Massy, France) equipped with an ESI⁺ source, operating in positive-ion mode. Source parameters were set as follows: capillary temperature at 320 °C, source voltage at 3500 V, sheath gas flow rate at 10 L min⁻¹. The divert valve was set to waste for the first 3 min. MS scans were operated in full-scan mode from m/z 100 to 1700 (0.1 s scan time) with a mass resolution of 11 000 at m/z 922. MS¹ scan was followed by MS² scans of the three most intense ions above an absolute threshold of 5000 counts. Selected parent ions were fragmented with on collision energie fixed at 50 eV and an isolation window of 1.3 amu. Calibration solution, containing two internal reference masses (purine, C₅H₄N₄, m/z 121.050873, and HP-921 [hexakis-(1*H*,1*H*,3*H*-tetrafluoropentoxy)phosphazene], C₁₈H₁₈O₆N₃P₃F₂₄, m/z 922.0098). A permanent MS/MS exclusion list criterion was set to prevent oversampling of the internal calibrants. LC-UV and MS data acquisition and processing were performed using MassHunter Workstation software (Agilent Technologies, Massy, France).

Molecular networking

The MS² data files related to the alkaloid extract of the barks of *V. africana* were converted from the .d (Agilent) standard data-format to .mzXML format using the MSConvert software, part of the ProteoWizard package.³⁹ A molecular network was created using the online Molecular Networking workflow (version release_8) at GNPS¹⁷ (<http://gnps.ucsd.edu>) with a parent mass tolerance of 0.02 Da and a MS/MS fragment ion tolerance of 0.02 Da. A network was then created where edges were filtered to have a cosine score above 0.65 and more than 6 matched peaks. Further edges between two nodes were kept in the network if and only if each of the nodes appeared in each other's respective top 10 most similar nodes. The spectra in the network were then searched against GNPS spectral libraries. All matches kept between network spectra and library spectra were required to have a score above 0.6 and at least 6 matched peaks. The molecular networking data were analyzed and visualized using Cytoscape (ver. 3.6.0).⁴⁰

Computational methods

The lowest energy conformer of compound **1** was fully optimized *in vacuo* and without constraint using DFT^{41,42} with the hybrid Becke-3-parameter-Lee-Yang-Parr^{43,44} exchange– correlation functional and the 6-31G* basis,⁴⁵ as implemented in the Gaussian 16 revB.01 software package.⁴⁶ Upon geometrical optimization convergence, a frequency calculation within the harmonic approximation was conducted at the same level of theory and conformer was characterized as a minimum by the absence of imaginary frequency. TDDFT at the same level of theory was then employed to predict energies as well as rotational strengths of the first 60 electronic transitions. The UCSF Chimera v1.11⁴⁷ software package was used for the depiction of the most stable conformer of compound **1**. ECD spectrum envelope was then calculated using SpecDis v1.71⁴⁸ using sigma/gamma value of 0.2 eV and a shift of +14 nm and rendered using Gnuplot v5.2.⁴⁹

Biological evaluation

Antibacterial activity assay by microdilutions. The antibacterial activity was assessed as previously described⁵⁰ against *Staphylococcus aureus* (ATCC 6538), *Pseudomonas aeruginosa* (ATCC 15442), *Mycobacterium smegmatis* (CIP 7326) and *Mycobacterium abscessus* (*M. abscessus* subsp. *bolletii*, ITM-M001006, BCCM, Belgium). The assays were performed in 96-well plates using a broth microdilution method in order to identify the minimal inhibitory concentration (MIC). Two-fold serial dilutions (100 μ L in 200 μ L final volume) of the molecules were first performed in triplicates in Mueller Hinton broth (or in the 7H9 medium when working with *M. abscessus*). Then, 100 μ L bacteria (100 fold dilution of 0.5 Mc Farland) were added into each well. Negative (without bacteria) and positive (without additional compounds) controls were present in each plate. The MIC value were first interpreted after 24 h incubation at 37 °C (or 2–3 days incubation for *M. abscessus*), corresponding to the lowest concentration inhibiting bacteria growth after visual inspection. This visual interpretation was always verified by adding MTT reagent, 3-(4,5-dimethylthiazol-2-yl)-2,5-diphenyltetrazolium bromide, (0.5 mg mL⁻¹ final concentration) to allow formazan crystal formation in viable cells during 4 h additional incubation period. A final naked eye inspection was performed to record the results. This assay was performed in triplicate in three separate experiments. Positive control drugs were vancomycin hydrochloride for *Staphylococcus aureus*, ceftrimide for *Pseudomonas aeruginosa*, and rifampicin for *Mycobacterium smegmatis*.

Activity assay against *M. bovis* BCG. To assess the antimycobacterial activity of our compounds on *M. bovis* BCG, the MIC was assessed by the microdilution method as previously described,⁵¹ performed in 7H9 medium supplemented with 10% albumin-dextrose complex and 0.2% glycerol in a polycarbonate tube to reach a final volume of 1 ml. Briefly, 0.5 mL of 2-fold serial drug dilutions were inoculated with 0.5 mL (at 5×10^5 CFU per mL) early exponential culture. Vancomycin at a final concentration of $25 \mu\text{g mL}^{-1}$ (far under its MIC $> 500 \text{ mg mL}^{-1}$) was eventually added to investigate the possible synergy between the two drugs. The MIC was interpreted as the lowest drug concentration that inhibited visible bacterial growth, defined by clump formation, when growth of the 1% inoculum drug-free control became visible (after 5–10 days growth).

The antimycobacterial activity was further assessed to investigate whether at the MIC, compounds could have an irreversible antimycobacterial activity (bactericidal activity) or a reversible effect (bacteriostatic activity) on *M. bovis* BCG. This was assessed by spreading $10 \mu\text{L}$ out of the 1 mL tubes from the broth microdilution method on 7H11 agar plate. Proliferation of bacteria colonies was interpreted as bacteria having encountered mycobacteriostatic compounds at their MIC, while absence of proliferation was interpreted as bacteria having encountered mycobactericidal compounds at their MBC (minimal bactericidal concentration).

Author contributions

The manuscript was written through contributions of all authors. All authors have given approval to the final version of the manuscript.

Conflicts of interest

There are no conflicts to declare.

Acknowledgements

We are very grateful to OPCW (Organisation for the Prohibition of Chemical Weapons) for the postdoctoral fellowship of H. F. and the financial support from ARES-CCD (Belgium). In addition, this work was supported by the French ANR grant ANR-20-CE43-0010. Leo Goehrs (Alionis) is gratefully acknowledged for the donation of the computing hardware.

Notes and references

1. Q. Zhao, W.-T. Zhu, X. Ding, Z.-Q. Huo, P. O. Donkor, T. A. Adelakun, X.-J. Hao and Y. Zhang, Voacafrines A-N, aspidosperma-type monoterpenoid indole alkaloids from *Voacanga africana* with AChE inhibitory activity, *Phytochemistry*, 2021, **181**, 112566 [CrossRef](#) [CAS](#) [PubMed](#).
2. M. Harada, K. N. Asaba, M. Iwai, N. Kogure, M. Kitajima and H. Takayama, Asymmetric Total Synthesis of an Iboga-Type Indole Alkaloid, Voacangalactone, Newly Isolated from *Voacanga africana*, *Org. Lett.*, 2012, **14**, 5800–5803 [CrossRef](#) [CAS](#) [PubMed](#).
3. C.-F. Ding, H.-X. Ma, J. Yang, X.-J. Qin, G. S. S. Njateng, H.-F. Yu, X. Wei, Y.-P. Liu, W.-Y. Huang, Z.-F. Yang, X.-H. Wang and X.-D. Luo, Antibacterial Indole Alkaloids with Complex Heterocycles from *Voacanga africana*, *Org. Lett.*, 2018, **20**, 2702–2706 [CrossRef](#) [CAS](#) [PubMed](#).
4. M. A. Beniddir, K. B. Kang, G. Genta-Jouve, F. Huber, S. Rogers and J. J. J. van der Hooft, , Advances in decomposing complex metabolite mixtures using substructure- and network-based computational metabolomics approaches, *Nat. Prod. Rep.*, 2021 [10.1039/D1NP00023C](#).
5. A. E. Fox Ramos, L. Evanno, E. Poupon, P. Champy and M. A. Beniddir, Natural products targeting strategies involving molecular networking: different manners, one goal, *Nat. Prod. Rep.*, 2019, **36**, 960–980 [RSC](#).
6. E. Otogo N'Nang, P. Le Pogam, T. Ndong Mba, C. Sima Obiang, E. Mouray, P. Grellier, B. Kumulungui, P. Champy and M. A. Beniddir, Targeted Isolation of Hemitheion from *Mostuea brunonis*, a Proposed Biosynthetic Intermediate of Theionbrunonines, *J. Nat. Prod.*, 2021, **84**, 1409–1413 [CrossRef](#).

7. T. Kouamé, G. Bernadat, V. Turpin, M. Litaudon, A. T. Okpekon, J.-F. Gallard, K. Leblanc, S. Rharrabti, P. Champy, E. Poupon, M. A. Beniddir and P. Le Pogam, Structure Reassignment of Melonine and Quantum-Chemical Calculations-Based Assessment of Biosynthetic Scenarios Leading to Its Revised and Original Structures, *Org. Lett.*, 2021, **23**, 5964–5968 [CrossRef](#).
8. C. F. Alcover, G. Bernadat, F. A. Kabran, P. Le Pogam, K. Leblanc, A. E. Fox Ramos, J.-F. Gallard, E. Mouray, P. Grellier, E. Poupon and M. A. Beniddir, Molecular Networking Reveals Serpentinine-Related Bisindole Alkaloids from *Picralima nitida*, a Previously Well- Investigated Species, *J. Nat. Prod.*, 2020, **83**, 1207–1216 [CrossRef](#) [CAS](#).
9. T. Kouamé, A. T. Okpekon, N. F. Bony, A. D. N'Tamon, J.-F. Gallard, S. Rharrabti, K. Leblanc, E. Mouray, P. Grellier, P. Champy, M. A. Beniddir and P. Le Pogam, Corynanthean-Epicatechin Flavoalkaloids from *Corynanthe pachyceras*, *Molecules*, 2020, **25**, 2654 [CrossRef](#).
10. G. Cauchie, E. O. N'Nang, J. J. J. van der Hooft, P. Le Pogam, G. Bernadat, J.-F. Gallard, B. Kumulungui, P. Champy, E. Poupon and M. A. Beniddir, Phenylpropane as an Alternative Dearomatizing Unit of Indoles: Discovery of Inaequalisines A and B Using Substructure-Informed Molecular Networking, *Org. Lett.*, 2020, **22**, 6077–6081 [CrossRef](#) [CAS](#).
11. A. D. N'Tamon, A. T. Okpekon, N. F. Bony, G. Bernadat, J.-F. Gallard, T. Kouamé, B. Séon-Méniel, K. Leblanc, S. Rharrabti, E. Mouray, P. Grellier, M. Ake, N. C. C. Amin, P. Champy, M. A. Beniddir and P. Le Pogam, Streamlined targeting of Amaryllidaceae alkaloids from the bulbs of *Crinum scillifolium* using spectrometric and taxonomically-informed scoring metabolite annotations, *Phytochemistry*, 2020, **179**, 112485 [CrossRef](#) [PubMed](#).
12. A. E. Fox Ramos, C. Pavesi, M. Litaudon, V. Dumontet, E. Poupon, P. Champy, G. Genta-Jouve and M. A. Beniddir, CANPA: Computer-Assisted Natural Products Anticipation, *Anal. Chem.*, 2019, **91**, 11247–11252 [CrossRef](#) [CAS](#) [PubMed](#).
13. A. E. Fox Ramos, P. Le Pogam, C. Fox Alcover, E. Ootogo N'Nang, G. Cauchie, H. Hazni, K. Awang, D. Bréard, A. M. Echavarren, M. Frédérick, T. Gaslonde, M. Girardot, R. Grougnet, M. S. Kirillova, M. Kritsanida, C. Lémus, A.-M. Le Ray, G. Lewin, M. Litaudon, L. Mambu, S. Michel, F. M. Miloserdov, M. E. Muratore, P. Richomme-Peniguel, F. Roussi, L. Evanno, E. Poupon, P. Champy and M. A.

- Beniddir, Collected mass spectrometry data on monoterpene indole alkaloids from natural product chemistry research, *Sci. Data*, 2019, **6**, 15 [CrossRef](#).
14. G. Baudouin, F. Tillequin, M. Bert and M. Koch, Ceridimine: a novel type of bisindole monoterpene alkaloid, *J. Chem. Soc., Chem. Commun.*, 1986, 3–4 [RSC](#).
15. T.-S. Kam and Y.-M. Choo, in *The Alkaloids: Chemistry and Biology*, ed. G. A. Cordell, Academic Press, 2006, vol. 63, pp. 181–337 [Search PubMed](#).
16. M. Kitajima and H. Takayama, in *The Alkaloids: Chemistry and Biology*, ed. H.-J. Knölker, Academic Press, 2016, vol. 76, pp. 259–310 [Search PubMed](#).
17. M. Wang, J. J. Carver, V. V. Phelan, L. M. Sanchez, N. Garg, Y. Peng, D. D. Nguyen, J. Watrous, C. A. Kapon, T. Luzzatto-Knaan, C. Porto, A. Bouslimani, A. V. Melnik, M. J. Meehan, W.-T. Liu, M. Crusemann, P. D. Boudreau, E. Esquenazi, M. Sandoval-Calderon, R. D. Kersten, L. A. Pace, R. A. Quinn, K. R. Duncan, C.-C. Hsu, D. J. Floros, R. G. Gavilan, K. Kleigrew, T. Northen, R. J. Dutton, D. Parrot, E. E. Carlson, B. Aigle, C. F. Michelsen, L. Jelsbak, C. Sohlenkamp, P. Pevzner, A. Edlund, J. McLean, J. Piel, B. T. Murphy, L. Gerwick, C.-C. Liaw, Y.-L. Yang, H.-U. Humpfer, M. Maansson, R. A. Keyzers, A. C. Sims, A. R. Johnson, A. M. Sidebottom, B. E. Sedio, A. Klitgaard, C. B. Larson, C. A. Boya P, D. Torres-Mendoza, D. J. Gonzalez, D. B. Silva, L. M. Marques, D. P. Demarque, E. Pociute, E. C. O'Neill, E. Briand, E. J. N. Helfrich, E. A. Granatosky, E. Glukhov, F. Ryffel, H. Houson, H. Mohimani, J. J. Kharbush, Y. Zeng, J. A. Vorholt, K. L. Kurita, P. Charusanti, K. L. McPhail, K. F. Nielsen, L. Vuong, M. Elfeki, M. F. Traxler, N. Engene, N. Koyama, O. B. Vining, R. Baric, R. R. Silva, S. J. Mascuch, S. Tomasi, S. Jenkins, V. Macherla, T. Hoffman, V. Agarwal, P. G. Williams, J. Dai, R. Neupane, J. Gurr, A. M. C. Rodriguez, A. Lamsa, C. Zhang, K. Dorrestein, B. M. Duggan, J. Almaliti, P.-M. Allard, P. Phapale, L.-F. Nothias, T. Alexandrov, M. Litaudon, J.-L. Wolfender, J. E. Kyle, T. O. Metz, T. Peryea, D.-T. Nguyen, D. VanLeer, P. Shinn, A. Jadhav, R. Muller, K. M. Waters, W. Shi, X. Liu, L. Zhang, R. Knight, P. R. Jensen, B. O. Palsson, K. Pogliano, R. G. Lington, M. Gutierrez, N. P. Lopes, W. H. Gerwick, B. S. Moore, P. C. Dorrestein and N. Bandeira, Sharing and community curation of mass spectrometry data with Global Natural Products Social Molecular Networking, *Nat. Biotechnol.*, 2016, **34**, 828–837 [CrossRef](#) [CAS](#).

18. DNP <http://dnp.chemnetbase.com/> (accessed Aug 27, 2021).
19. H. Takayama, S. Suda, I.-S. Chen, M. Kitajima, N. Aimi and S.-i. Sakai, Two New Dimeric Indole Alkaloids from *Tabernaemontana subglobosa* Merr. from Taiwan, *Chem. Pharm. Bull.*, 1994, **42**, 280–284 [CrossRef](#) [CAS](#).
20. M. Azoug, A. Loukaci, B. Richard, J.-M. Nuzillard, C. Moreti, M. Zèches-Hanrot and L. Le Men-Olivier, Alkaloids from stem bark and leaves of *Peschiera buchtieni*, *Phytochemistry*, 1995, **39**, 1223–1228 [CrossRef](#) [CAS](#).
21. S. Subhadhirasakul, H. Takayama, Y. Miyabe, M. Kitajima, D. Ponglux, S.-i. Sakai and N. Aimi, Two novel sarpagine-type indole alkaloids from the leaves of *Hunteria zeylanica* in Thailand, *Heterocycles*, 1995, **9**, 2049–2056 [Search PubMed](#).
22. T.-S. Kam and K.-M. Sim, Conodurine, conoduramine, and ervahanine derivatives from *Tabernaemontana corymbosa*, *Phytochemistry*, 2003, **63**, 625–629 [CrossRef](#) [CAS](#) [PubMed](#).
23. C. Zhang, Y. Idelbayev, N. Roberts, Y. Tao, Y. Nannapaneni, B. M. Duggan, J. Min, E. C. Lin, E. C. Gerwick, G. W. Cottrell and W. H. Gerwick, Small Molecule Accurate Recognition Technology (SMART) to Enhance Natural Products Research, *Sci. Rep.*, 2017, **7**, 14243 [CrossRef](#) [PubMed](#).
24. R. Reher, H. W. Kim, C. Zhang, H. H. Mao, M. Wang, L.-F. Nothias, A. M. Caraballo-Rodriguez, E. Glukhov, B. Teke, T. Leao, K. L. Alexander, B. M. Duggan, E. L. Van Everbroeck, P. C. Dorrestein, G. W. Cottrell and W. H. Gerwick, A Convolutional Neural Network-Based Approach for the Rapid Annotation of Molecularly Diverse Natural Products, *J. Am. Chem. Soc.*, 2020, **142**, 4114–4120 [CrossRef](#) [CAS](#) [PubMed](#).
25. T. M. Zennie, J. M. Cassady and R. F. Raffaui, Funebral, a New Pyrrole Lactone Alkaloid from *Quararibea funebris*, *J. Nat. Prod.*, 1986, **49**, 695–698 [CrossRef](#) [CAS](#).
26. N. Harada and K. Nakanishi, Exciton chirality method and its application to configurational and conformational studies of natural products, *Acc. Chem. Res.*, 1972, **5**, 257–263 [CrossRef](#) [CAS](#).
27. A. E. Nugroho, Y. Hirasawa, N. Kawahara, Y. Goda, K. Awang, A. H. A. Hadi and H. Morita, Bisnicalaterine A, a Vobasine–Vobasine Bisindole Alkaloid from *Hunteria zeylanica*, *J. Nat. Prod.*, 2009, **72**, 1502–1506 [CrossRef](#) [CAS](#).

28. J. Xu, Y. C. Song, Y. Guo, Y. N. Mei and R. X. Tan, Fumigaclavines D–H, New Ergot Alkaloids from Endophytic *Aspergillus fumigatus*, *Planta Med.*, 2014, **80**, 1131–1137 [CrossRef](#) [CAS](#).
29. C. K. Narkowicz, A. J. Blackman, E. Lacey, J. H. Gill and K. Heiland, Convolutindole A and Convolutamine H, New Nematocidal Brominated Alkaloids from the Marine Bryozoan *Amathia convoluta*, *J. Nat. Prod.*, 2002, **65**, 938–941 [CrossRef](#) [CAS](#).
30. L. S. Mulwa, R. Jansen, D. F. Praditya, K. I. Mohr, J. Wink, E. Steinmann and M. Stadler, Six Heterocyclic Metabolites from the Myxobacterium *Labilithrix luteola*, *Molecules*, 2018, **23**, 542 [CrossRef](#).
31. T. A. Foderaro, L. R. Barrows, P. Lassota and C. M. Ireland, Bengacarboline, a New β -Carboline from a Marine Ascidian *Didemnum* sp., *J. Chem. Org.*, 1997, **62**, 6064–6065 [CrossRef](#) [CAS](#).
32. A. M. Wolters, D. A. Jayawickrama and J. V. Sweedler, Comparative Analysis of a Neurotoxin from *Calliostoma canaliculatum* by On-Line Capillary Isotachopheresis/H NMR and Diffusion ^1H NMR, *J. Nat. Prod.*, 2005, **68**, 162–167 [CrossRef](#) [CAS](#) [PubMed](#).
33. C. T. Walsh, Biological Matching of Chemical Reactivity: Pairing Indole Nucleophilicity with Electrophilic Isoprenoids, *ACS Chem. Biol.*, 2014, **9**, 2718–2728 [CrossRef](#) [CAS](#).
34. M. E. Tanner, Mechanistic studies on the indole prenyltransferases, *Nat. Prod. Rep.*, 2015, **32**, 88–101 [RSC](#).
35. J. M. Wood, D. P. Furkert and M. A. Brimble, 2-Formylpyrrole natural products: origin, structural diversity, bioactivity and synthesis, *Nat. Prod. Rep.*, 2019, **36**, 289–306 [RSC](#).
36. M. Hellwig and T. Henle, Baking, Ageing, Diabetes: A Short History of the Maillard Reaction, *Angew. Chem., Int. Ed.*, 2014, **53**, 10316–10329 [CrossRef](#) [CAS](#).
37. W.-G. Shan, Y. Wang, L.-F. Ma and Z.-J. Zhan, A new pyrrole alkaloid from the mycelium of *Inonotus obliquus*, *J. Chem. Res.*, 2017, **41**, 392–393 [CrossRef](#) [CAS](#).
38. Z. Sun, M. Hu, Z. Sun, N. Zhu, J. Yang, G. Ma and X. Xu, Pyrrole Alkaloids from the Edible Mushroom *Phlebopus portentosus* with Their Bioactive Activities, *Molecules*, 2018, **23**, 1198 [CrossRef](#).

39. M. C. Chambers, B. Maclean, R. Burke, D. Amodei, D. L. Ruderman, S. Neumann, L. Gatto, B. Fischer, B. Pratt, J. Egertson, K. Hoff, D. Kessner, N. Tasman, N. Shulman, B. Frewen, T. A. Baker, M.-Y. Brusniak, C. Paulse, D. Creasy, L. Flashner, K. Kani, C. Moulding, S. L. Seymour, L. M. Nuwaysir, B. Lefebvre, F. Kuhlmann, J. Roark, P. Rainer, S. Detlev, T. Hemenway, A. Huhmer, J. Langridge, B. Connolly, T. Chadick, K. Holly, J. Eckels, E. W. Deutsch, R. L. Moritz, J. E. Katz, D. B. Agus, M. MacCoss, D. L. Tabb and P. Mallick, A cross-platform toolkit for mass spectrometry and proteomics, *Nat. Biotechnol.*, 2012, **30**, 918–920 [CrossRef](#) [CAS](#).
40. P. Shannon, A. Markiel, O. Ozier, N. S. Baliga, J. T. Wang, D. Ramage, N. Amin, B. Schwikowski and T. Ideker, Cytoscape: A Software Environment for Integrated Models of Biomolecular Interaction Networks, *Genome Res.*, 2003, **13**, 2498–2504 [CrossRef](#) [CAS](#).
41. P. Hohenberg and W. Kohn, Inhomogeneous Electron Gas, *Phys. Rev.*, 1964, **136**, B864–B871 [CrossRef](#).
42. W. Kohn and L. J. Sham, Self-Consistent Equations Including Exchange and Correlation Effects, *Phys. Rev. [Sect.] B*, 1965, **140**, A1133–A1138 [CrossRef](#).
43. A. D. Becke, Density–functional thermochemistry. III. The role of exact exchange, *J. Chem. Phys.*, 1993, **98**, 5648–5652 [CrossRef](#) [CAS](#).
44. C. Lee, W. Yang and R. G. Parr, Development of the Colle-Salvetti correlation-energy formula into a functional of the electron density, *Phys. Rev. B: Condens. Matter Mater. Phys.*, 1988, **37**, 785–789 [CrossRef](#) [CAS](#).
45. W. J. R. Hehre, L. Radom, P. V. R. Schleyer and J. A. Pople, *AB Initio Molecular Orbital Theory*, Wiley, New York, 1986 [Search PubMed](#).
46. M. J. Frisch, H. B. Trucks, G. W. Schlegel, G. E. Scuseria, M. A. Robb, J. R. Cheeseman, G. Scalmani, V. Barone, G. A. Petersson and H. Nakatsuji, *et al. Gaussian 16 Revision B.01*, Gaussian Inc., Wallingford, CT, USA, 2016 [Search PubMed](#).
47. E. F. Pettersen, T. D. Goddard, C. C. Huang, G. S. Couch, D. M. Greenblatt, E. C. Meng and T. E. Ferrin, UCSF Chimera—A visualization system for exploratory research and analysis, *J. Comput. Chem.*, 2004, **25**, 1605–1612 [CrossRef](#) [CAS](#) [PubMed](#).
48. T. Bruhn, A. Schaumlöffel, Y. Hemberger and G. Bringmann, SpecDis: Quantifying the Comparison of Calculated and Experimental Electronic Circular Dichroism Spectra, *Chirality*, 2013, **25**, 243–249 [CrossRef](#) [CAS](#).

49. H. B. Bröker, J. Campbell, R. Cunningham, D. Denholm, G. Elber, R. Fearick, C. Grammes, L. Hart, L. Heckingu and P. Juhász, *Gnuplot 4.6: an Interactive Plotting Program*, <http://gnuplot.sourceforge.net/> [Search PubMed](#).
50. S. Oliveira Ribeiro, V. Fontaine, V. Mathieu, A. Zhiri, D. Baudoux, C. Stévigny and F. Souard, Antibacterial and Cytotoxic Activities of Ten Commercially Available Essential Oils, *Antibiotics*, 2020, **9**, 717 [CrossRef](#).
51. C. Rens, F. Laval, M. Daffé, O. Denis, R. Frita, A. Baulard, R. Wattiez, P. Lefèvre and V. Fontaine, Effects of Lipid-Lowering Drugs on Vancomycin Susceptibility of Mycobacteria, *Antimicrob. Agents Chemother.*, 2016, **60**, 6193–6199 [CrossRef](#) [CAS](#).
-

Footnote

† Electronic supplementary information (ESI) available: Cartesian coordinates, HRMS, and NMR data of **1**. See DOI: [10.1039/d1ob01791h](https://doi.org/10.1039/d1ob01791h)

This journal is © The Royal Society of Chemistry 2022